NUMERICAL MODELING OF SPACE PLASMA FLOWS: ASTRONUM-2008
ASP Conference Series, Vol. 406, 2009
Nikolai V. Pogorelov, Edouard Audit, Phillip Colella, and Gary P. Zank, eds.

Simulations of Supersonic Turbulence in Molecular Clouds: Evidence for a New Universality

A. G. Kritsuk[1], S. D. Ustyugov[2], M. L. Norman[3], and P. Padoan[3]

Abstract. We use three-dimensional simulations to study the statistics of supersonic turbulence in molecular clouds. Our numerical experiments describe driven turbulent flows with an isothermal equation of state, Mach numbers around 10, and various degrees of magnetization. We first support the so-called 1/3-rule of Kritsuk et al. (2007a) with our new data from a larger 2048^3 simulation. We then attempt to extend the 1/3-rule to supersonic MHD turbulence and get encouraging preliminary results based on a set of 512^3 simulations. Our results suggest an interesting new approach to tackle universal scaling relations and intermittency in supersonic MHD turbulence.

1. Introduction

Supersonic turbulence plays an important role in shaping hierarchical internal substructure of molecular clouds (MCs). Since the process of star formation begins with the formation of dense cores, turbulence can be responsible for creating initial conditions for star formation. It is hard to access the supersonic regimes typical for MC turbulence in the laboratory and the information available from observations is also limited. Thus numerical simulations currently represent the only way to explore the statistics of supersonic turbulence, the key ingredient of any successful statistical theory of star formation (Padoan et al. 2007; McKee & Ostriker 2007). For a long time, the nature of *highly compressible* and *magnetized* interstellar turbulence remained poorly understood. We use large-scale numerical simulations to shed light on the energy transfer between scales and on the key spatial correlations of relevant fields in these flows.

2. The 1/3-rule for Supersonic Hydrodynamic Turbulence

In Kritsuk et al. (2007a, hereafter K07) we showed that homogeneous isotropic turbulence in a strongly compressible regime typical for the interstellar gas can be approximated by modified Kolmogorov's laws since nonlinear advection still remains the major physical process at work in the absence of magnetic fields. The essence of the required modification boils down to the use of proper density

[1]Center for Ap. & Sp. Sci., UC San Diego, 9500 Gilman Drive, La Jolla, CA 92093-0424, USA; Department of Math. & Mech., St. Petersburg State University, St. Petersburg 198504, Russia

[2]Keldysh Institute for Applied Mathematics, Russian Academy of Sciences, Miusskaya Pl. 4, Moscow 125047, Russia

[3]Physics Department, UC San Diego, 9500 Gilman Drive, La Jolla, CA 92093-0424, USA

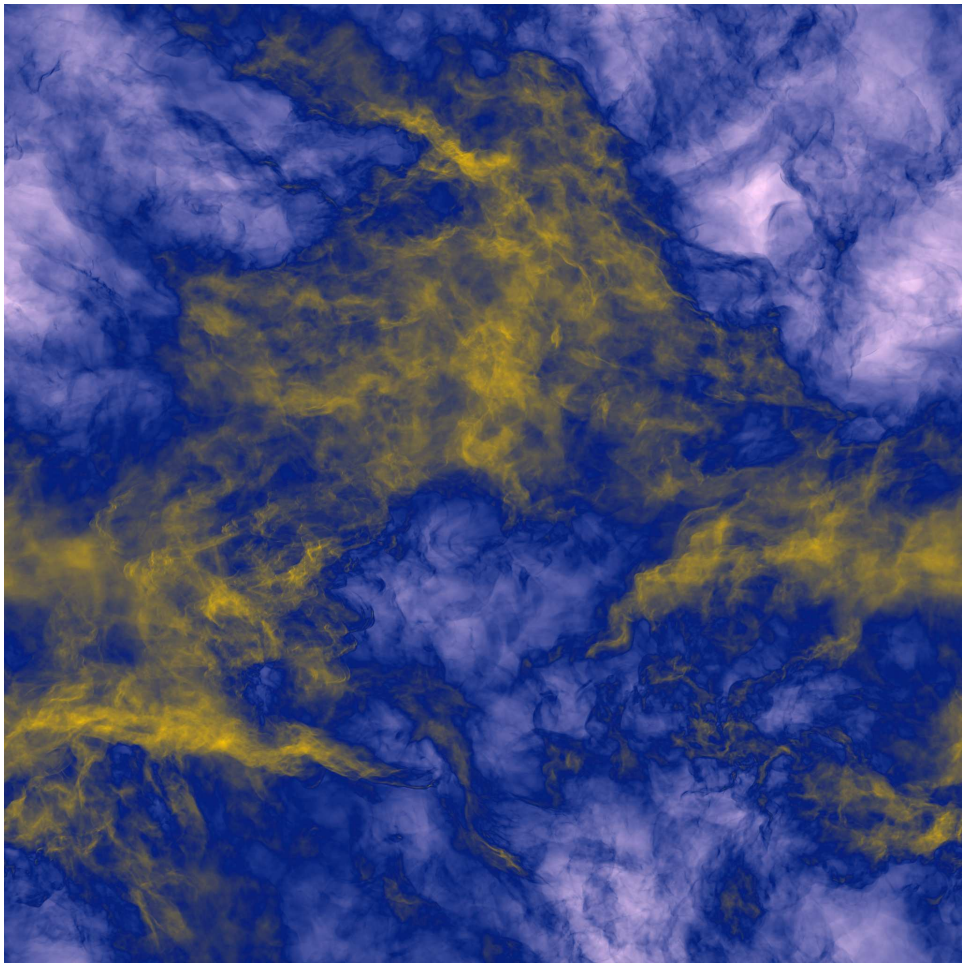

Figure 1. A snapshot of the projected gas density from the 2048^3 Mach 6 turbulence simulation with PPM. White-blue-yellow colors correspond to low-intermediate-high projected density values.

weighting for the gas velocity, which we call the "1/3-rule" of supersonic turbulence. Replacing the velocity $\mathbf{u}$ by $\rho^{1/3}\mathbf{u}$, one can show that for this quantity the 4/5-law of Kolmogorov (1941) approximately holds at sonic Mach number as large as $M_s = 6$, when the plain velocity power spectrum already scales as in Burgers turbulence, i.e. $\sim k^2$. The first von Kármán–Howarth (1938) relation between the second-order transverse and longitudinal velocity structure functions also still holds approximately at $M_s = 6$. Although there is no rigorous proof for any of these two fundamental exact incompressible laws in supersonic regimes, the evidence provided by numerical experiments helps extend Kolmogorov's phenomenology to a wider class of problems of interest in turbulence research and astrophysics. In K07 we showed that the low-order statistics of $\rho^{1/3}\mathbf{u}$ are invariant with respect to changes in the Mach number. For instance, the slope of the power spectrum is -1.69, and the exponent of the third-order structure function $S_3(\ell)$ is unity, $S_3(\ell) \equiv \langle|\delta u(\ell)|^3\rangle \sim \ell$.

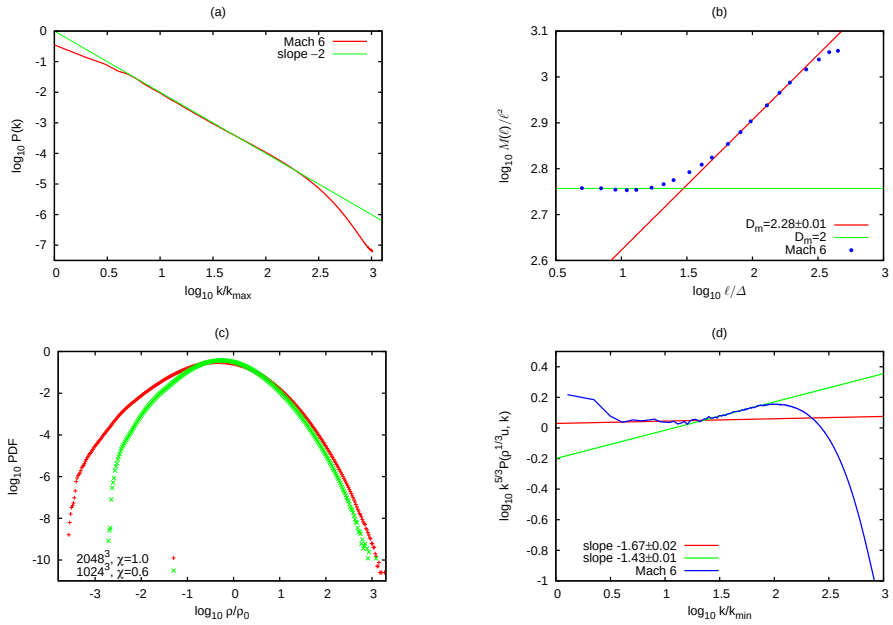

Figure 2. Statistics of supersonic turbulence from the 2048^3 simulation at $M_s = 6$: (**a**) power spectrum of projected density (an ensemble average over 1275 projections); (**b**) average gas mass $M(\ell)$ for boxes centered around the highest density peaks as a function of box size, the horizontal line corresponds to a fractal mass dimension $D_m = 2$; (**c**) density pdfs for the 2048^3 simulation with a solenoidal driving force ($\chi = 1$) and for 1024^3 simulation with a hybrid driving ($\chi = 0.6$, K07); (**d**) compensated power spectrum of $\rho^{1/3}\mathbf{u}$.

Here we report on our more recent simulation with a grid resolution of 2048^3 carried out with the ENZO code on *Bigben* (PSC) and on *Ranger* (TACC) using 4096 cores (Fig. 1). The simulation details can be found in K07, except that this new run employs a purely solenoidal large-scale driving force.

Turbulence statistics derived from these new data with unprecedented dynamic range confirm the convergence of our earlier results obtained with lower resolution. Figure 2 provides a brief summary of the new statistics. The power spectrum of projected gas density has a slope of -2.01 ± 0.01 in the inertial range, consistent with the 3D density power index of -1.07 ± 0.01 reported in K07 (Fig. 2**a**). The slopes of the power spectra of density and log density (not shown) are very close to -1 and to $-5/3$, respectively. However, it is a mere coincidence that at Mach 6 the slopes are represented by these "good" numbers, since already at $M_s = 10$ they become shallower. Our new estimate for the "fractal" dimension of the density distribution for the inertial range of Mach 6 turbulence, $D_m \approx 2.3$, agrees well with the previously obtained value of 2.4 (Fig. 2**b**, see K07 for definition details). In the dissipation range, where individual shock fronts are the dominant structures, $D_m = 2$ (cf. Kritsuk et al. 2007b; Schmidt et al. 2008; Pan et al. 2009; Schmidt et al. 2009). Figure 2**c** compares the probability density functions (pdfs) of the gas density from simulations with different driving forces. Both cases agree nicely with lognormal distributions at high densities and show some divergence at low densities that can be at least

partly attributed to poor statistical representation of violently evolving rarefactions due to a limited number of flow snapshots used to derive the pdfs (100 for the 2048^3 data and 170 for K07 data), cf. Lemaster & Stone (2008); Federrath et al. (2008). Finally, Fig. 2**d** shows a sample power spectrum of $\rho^{1/3}\mathbf{u}$ that also confirms the scaling obtained in K07 based on a lower resolution simulations.

3. New Scaling Laws for Supersonic MHD Turbulence

We carried out a set of pilot simulations of driven isothermal supersonic turbulence at the sonic Mach number of 10 on 512^3 meshes to demonstrate the performance of our new PPML solver for ideal MHD (Popov & Ustyugov 2007, 2008; Ustyugov et al. 2009). The models are initiated with a uniform magnetic field aligned with the x-coordinate direction and cover the transition to turbulence and its evolution for up to 10 dynamical times. A large-scale ($k \leq 2$) nonhelical solenoidal force is used to stir the gas in the periodic domain which keeps M_s close to 10 during the simulation, see Fig. 3**a**. The magnetic field is not forced and can receive energy only through interaction with the velocity field. This random forcing does not generate a mean field, but still leads to amplification of the small-scale magnetic energy via a process known as small-scale dynamo (Schekochihin & Cowley 2007, and references therein). It is implicitly assumed that the magnetic Prandtl number $Pm \approx 1$ in our numerical models. Each simulation reaches a steady state with saturated magnetic energy and a macroscopically statistically isotropic magnetic field, see Fig. 3**b**. The properties of this saturated state representing fully developed isotropic compressible MHD turbulence is the main focus of this section. While some level of physical understanding of small-scale dynamo and its saturation exists, the structure of the saturated state is poorly known, even in the incompressible case (Yousef et al. 2007).

Our models are parameterized by the ratios of thermal-to-magnetic pressure $\beta \equiv P_{gas}/P_{mag}$. The initial values $\beta_0 = 20$ and 2 translate into saturated levels of the magnetic energy at about 10% and 30% of the kinetic energy, respectively (Fig. 3**b**). In the $\beta_0 = 0.2$ case we get a statistical steady state with energy equipartition. The three simulations fully cover the transition from highly super-Alfvénic regime of turbulence at $\beta_0 = 20$ with the root mean square (rms) Alfvénic Mach number $M_A \approx 10$ through mildly super-Alfvénic ($\beta_0 = 2$, $M_A \approx 3$) to trans-Alfvénic ($\beta_0 = 0.2$, $M_A \approx 1$), see Fig. 3**a**. The mean normalized cross-helicity $\sigma_c \equiv 2\left\langle \mathbf{u}\cdot\mathbf{B}\right\rangle / (\left\langle \mathbf{u}^2\right\rangle + \left\langle \mathbf{B}^2\right\rangle)$ is contained within $\pm 1.5\%$ for $\beta_0 = 20$ and 2, while at $\beta_0 = 0.2$ the cross-helicity oscillates somewhat more actively with $\sigma_c \in (-0.073, 0.015)$. Still, to a good approximation, the turbulence remains nonhelical. In all three cases PPML keeps the divergence of the magnetic field at all times to within $|\nabla\cdot\mathbf{B}| < 10^{-12}$. We computed time-average statistics over at least four dynamical times for the saturated regimes. The results are discussed below.

The dependence of the density pdf on the value of β_0 shows a very clear trend for substantially weaker rarefactions in the flows with stronger magnetic field (smaller plasma β), see Fig. 3**c**. At a grid resolution of 512^3, the average minimum density is about $10^{-3.6}$, $10^{-2.7}$, and 10^{-2} for $\beta_0 = 20$, 2, and 0.2, respectively. At the same time, the high-density wing of the pdf preserves

its lognormal shape and appears insensitive to the intensity level of magnetic fluctuations within the studied range of β_0.

The density power spectra also show some trends with the magnetic field strength, although they are less pronounced than in the velocity spectra (see below). For example, the power spectrum of the logarithm of projected gas density scales as $k^{-1.79}$, $k^{-1.64}$, and $k^{-1.52}$ at $\beta_0 = 20$, 2, and 0.2, respectively (see also Sec. 2 above). The density spectrum for $\beta_0 = 20$ (nearly nonmagnetized medium) at $M_s = 10$ scales as $k^{-0.7}$, i.e. it is shallower than in our nonmagnetized simulations at $M_s = 6$, where the k^{-1} scaling was recovered. This result confirms K07 prediction that in the limit $M_s \to \infty$ the density spectrum is flat, $P(\rho, k) \sim k^0$, similar to the white noise spectrum. At a fixed sonic Mach number ($M_s = 10$), as the flow magnetization increases (M_A drops from 10 to 1), the density spectra tend to flatten, see Fig. 3**d**. The same tendency is clear in the power spectra of the logarithm of the density, with the slopes around -1.3 at $M_s = 10$. This is consistent with a slope of -1.7 we measured at $M_s = 6$ and $\beta_0 = \infty$. We also observe a significant reduction in the extent of the scaling interval in the $\log \rho$ spectra as β_0 decreases from 20 to 0.2.

We measured a broad range of the velocity power indices from -1.5 through -2 depending on the degree of magnetization (Fig. 3**e**). As expected, the highly super-Alfvénic case $\beta_0 = 20$ is very similar to K07 results for nonmagnetized flows, with a Burgers-like scaling of the velocity power spectrum, $P(\mathbf{u}, k) \sim k^{-1.94}$, and a Kolmogorov-like spectrum for the density-weighted velocity, $P(\rho^{1/3}\mathbf{u}, k) \sim k^{-1.7}$ (Fig. 3**f**, also see Kowal & Lazarian 2007). There is a clear trend for the velocity power spectra to get shallower at higher degrees of magnetization. We get $k^{-1.62}$ at $\beta_0 = 2$ and $k^{-1.51}$ at $\beta_0 = 0.2$, consistent with the Lemaster & Stone (2009) measurement for their strong-field case, $k^{-1.38}$ at $\beta_0 = 0.02$ and $M_s = 6.9$. This result suggests that slopes of the velocity power spectra around -1.8 inferred from the observations of molecular clouds (e.g., Padoan et al. 2006) may indicate a super-Alfvénic nature of the turbulence there, see however a related discussion in Li et al. (2008).

There is a set of exact scaling laws for homogeneous and isotropic incompressible MHD turbulence analogous to the 4/5-law of Kolmogorov for ordinary turbulence in neutral fluids (Chandrasekhar 1951; Politano & Pouquet 1998a,b). The MHD laws can be expressed in terms of Elsässer fields, $\mathbf{z}^{\pm} \equiv \mathbf{u} \pm \mathbf{B}/\sqrt{4\pi\rho}$ (Elsässer 1950), as $S^{\pm}_{\parallel,3} \equiv \left\langle \delta z^{\mp}_{\parallel}(\ell)[\delta z^{\pm}_{i}(\ell)]^2 \right\rangle = -\frac{4}{d}\epsilon^{\pm}\ell$, where $\delta\mathbf{z}_{\parallel}(\ell) \equiv [\mathbf{z}(\mathbf{x} + \hat{\mathbf{e}}\ell) - \mathbf{z}(\mathbf{x})] \cdot \hat{\mathbf{e}}$, d is the space dimension, $\hat{\mathbf{e}}$ is a unit vector with arbitrary direction, $\hat{\mathbf{e}}\ell$ is the displacement vector, the brackets denote an ensemble average, and summation over repeated indices is implied. Equivalently, the scaling laws can be rewritten in terms of the basic fields ($\mathbf{u}$, $\mathbf{B}$), but in MHD there are no separate *exact* laws for the velocity or the magnetic field alone. It is important not to neglect the correlations between the $\mathbf{u}$ and $\mathbf{B}$ fields or $\mathbf{z}^+$ and $\mathbf{z}^-$ fields constrained by the invariance properties of the equations in turbulent cascade models. In supersonic turbulence, it is equally important to properly account for the density–velocity and density–magnetic field correlations. In incompressible MHD, the total energy $\langle (u_i^2 + B_i^2)/2 \rangle$ and the cross-helicity $\langle \mathbf{u} \cdot \mathbf{B} \rangle$ play the role of ideal invariants and, thus, the (total) energy transfer rate $\epsilon^T = (\epsilon^+ + \epsilon^-)/2$ and the cross-helicity transfer rate $\epsilon^C = (\epsilon^+ - \epsilon^-)/2$. For vanishing magnetic field $\mathbf{B}$, one recovers the Kolmogorov

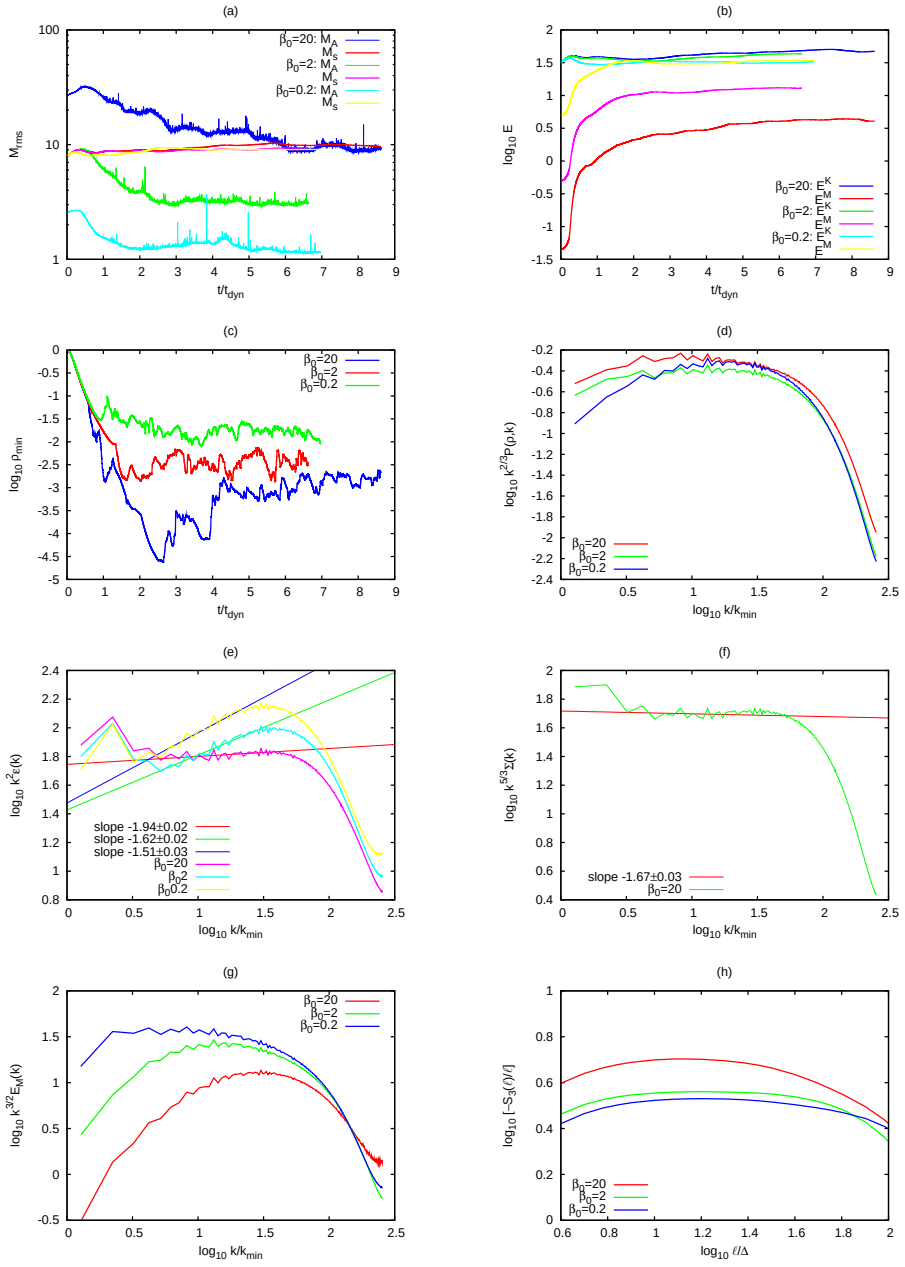

Figure 3. Statistics of MHD turbulence at $M_s = 10$ and $\beta_0 = 20$, 2, and 0.2 from PPML simulations at grid resolution of 512^3 points: (**a**) rms sonic and Alfvénic Mach numbers vs. time; (**b**) mean kinetic and magnetic energy vs. time; (**c**) minimum gas density vs. time; (**d**) time-average compensated density power spectra; (**e**) time-average compensated velocity power spectra; (**f**) time-average compensated power spectrum of $\rho^{1/3}\mathbf{u}$ for $\beta_0 = 20$; (**g**) time-average compensated power spectra of magnetic energy; (**h**) time-average compensated third-order structure functions $S_3(\ell)$ for generalized Elsaässer fields $\mathbf{Z}^{\pm}$, see text for the definition details.

4/5-law, $\langle[\delta\mathbf{u}_\parallel(\ell)]^3\rangle = -4/5\epsilon\ell$, where ϵ is the mean rate of kinetic energy transfer (Politano & Pouquet 1998b).

Numerical simulations generally confirm these incompressible scalings, although the Reynolds numbers are perhaps still too small to reproduce the asymptotic linear behavior with a desired precision and the results are sensitive to statistical errors (Biskamp & Müller 2000; Porter et al. 2002; Boldyrev et al. 2006). Often, the absolute value of the longitudinal difference is used and still a linear scaling is recovered numerically, while there is no rigorous result for the normalization constant in this case. The third-order transverse velocity structure functions also show a linear scaling in simulations of nonmagnetized turbulence (Porter et al. 2002, K07) and the difference of scaling exponents for longitudinal and transverse structure functions can serve as a robust measure of statistical uncertainty of the computed exponents (Kritsuk & Norman 2004). In MHD simulations, the third-order structure functions of the Elsässer fields $\left\langle|\delta z_\parallel^\mp(\ell)|^3\right\rangle$ were shown to have an approximately linear scaling too (Biskamp & Müller 2000; Momeni & Mahdizadeh 2008), but again there is no reason for this result to universally hold in all situations since the correlations between the $\mathbf{z}^\pm$ fields play an important role in nonlinear transfer processes.

Can the 4/3-law for incompressible MHD turbulence be extended to highly compressible supersonic regimes in molecular clouds? As we discussed above, a proper density weighting of the velocity, $\rho^{1/3}\mathbf{u}$, preserves the approximately linear scaling of the third-order structure functions at high Mach numbers in the nonmagnetized case (for a more involved approach to density weighting see Pan et al. 2009). It is straightforward to redefine the Elsaässer fields for compressible flows using the 1/3-rule, $\mathbf{Z}^\pm \equiv \rho^{1/3}(\mathbf{u} \pm \mathbf{B}/\sqrt{4\pi\rho})$, so that they match the original $\mathbf{z}^\pm$ fields in the incompressible limit and reduce to $\rho^{1/3}\mathbf{u}$ in the limit of vanishing $\mathbf{B}$. The new $\mathbf{Z}^\pm$ fields can have universal scaling properties in homogeneous isotropic turbulent flows with a broad range of sonic and Alfvénic Mach numbers.

We use data from our MHD simulations to find evidence to support or reject this conjecture by computing the third-order structure functions $S^\pm_{\parallel,3}$ and $S^\pm_{\perp,3}$ defined above, but now based on the new $\mathbf{Z}^\pm$ fields. Since we are interested in the energy transfer through the inertial interval, we compute the sum of $S^-_{\parallel,3}$ and $S^+_{\parallel,3}$ which determines the energy transfer rate ϵ^T in the incompressible limit. To further reduce statistical errors, we had to combine the transverse and longitudinal structure functions, but the absolute value operator was not applied to the field differences. The results are plotted in Fig. 3**h**, which shows the compensated scaling for $S_3(\ell) \equiv (S^-_{\parallel,3} + S^+_{\parallel,3} + S^-_{\perp,3} + S^+_{\perp,3})/4$ averaged over about two dozen snapshots for each of the three saturated turbulent states with different levels of magnetic fluctuations. Although the scaling range is rather short in 512^3 numerical data, each of the three cases clearly demonstrates a linear behavior $S_3(\ell) \sim \ell$, in contrast to the corresponding scaling of the velocity or the magnetic energy which strongly depend on β_0, see Fig. 3**e** and **g**. As a consistency check, we computed $\tilde{S}_3(\ell) \equiv (S^-_{\parallel,3}+S^+_{\parallel,3})/2$ for both plain $\mathbf{z}^\pm$ fields and for density-weighted $\mathbf{Z}^\pm$ fields at $\beta_0 = 2$. We then compared the scaling $\tilde{S}_3 \sim \ell^\alpha$ for the two cases and found that the plain Elsässer fields result in a steeper slope, $\Delta\alpha \equiv \alpha_\mathbf{z} - \alpha_\mathbf{Z} \approx 0.23$. K07 measured a similar slope difference, $\Delta\alpha \approx 0.31$,

for the third-order longitudinal velocity structure functions in nonmagnetized turbulence at $M_s = 6$.

While larger simulations are definitely needed to confirm the linear scaling, we believe that our preliminary evidence suggests an interesting new approach to tackle universal scaling relations and intermittency in compressible MHD turbulence.

4. Conclusions

We further supported the 1/3-rule of K07 for hydrodynamic supersonic turbulence with new data from a larger simulation at $M_s = 6$ on a grid of 2048^3 points. Based on a series of 512^3 MHD turbulence simulations at $M_s = 10$, we explored universal trends in scaling properties of various statistics as a function of the magnetic field strength. Our data suggest that the 4/3-law of incompressible MHD can be extended to supersonic flows.

Acknowledgments. This research was supported in part by the National Science Foundation through grants AST-0607675 and AST-0808184, as well as through TeraGrid resources provided by NICS, PSC, SDSC, and TACC (MCA07S014 and MCA98N020).

References

Chandrasekhar, S. 1951, Proc. Roy. Soc. London, Ser. A, 204, 435
Biskamp, D., Müller, W.-C. 2000, Physics of Plasmas, 7, 4889
Boldyrev, S., Mason, J., & Cattaneo, F. 2006, arXiv:astro-ph/0605233
Elsässer, W. M. 1950, Phys. Rev., 79, 183
Federrath, C., Klessen, R. S., & Schmidt, W. 2008, ApJ, 688, L79
Kolmogorov, A. N. 1941, Dokl. Acad. Nauk SSSR, 32, 19
Kowal, G., & Lazarian, A. 2007, ApJ, 666, L69
Kritsuk, A. G., Norman, M. L., Padoan, P., & Wagner, R. 2007a, ApJ, 665, 416 (**K07**)
Kritsuk, A., Padoan, P., Wagner, R., & Norman, M. 2007b, AIP Conf. Proc., 932, 393
Kritsuk, A. G., & Norman, M. L. 2004, ApJ, 601, L55
Lemaster, M. N., & Stone, J. M. 2009, ApJ, 691, 1092
Lemaster, M. N., & Stone, J. M. 2008, ApJ, 682, L97
Li, P. S., McKee, C. F., Klein, R. I., & Fisher, R. T. 2008, ApJ, 684, 380
McKee, C. F., & Ostriker, E. C. 2007, ARA&A, 45, 565
Momeni, M., & Mahdizadeh, N. 2008, Physica Scripta, T131, 014004
Padoan, P., Nordlund, Å., Kritsuk, A., Norman, M., & Li, P. S. 2007, ApJ, 661, 972
Padoan, P., Juvela, M., Kritsuk, A., & Norman, M. L. 2006, ApJ, 653, L125
Pan, L., Padoan, P., & Kritsuk, A. G. 2009, Phys. Rev. Lett., 102, 034501
Politano, H., & Pouquet, A. 1998a, Phys. Rev. E, 57, 21
Politano, H., & Pouquet, A. 1998b, Geoph. Res. Lett., 25, 273
Popov, M. V., & Ustyugov, S. D. 2008, Comp. Math. & Math. Phys., 48, 477
Popov, M. V., & Ustyugov, S. D. 2007, Comp. Math. & Math. Phys., 47, 1970
Porter, D., Pouquet, A., & Woodward, P. 2002, Phys. Rev. E, 66, 026301
Schekochihin, A. A. & Cowley, S. C. 2007, in: Molokov, S., Moreau, R., and Moffatt, H.K. (Eds.), Magnetohydrodynamics: Historical Evolution and Trends, 85
Schmidt, W., Federrath, C., Hupp, M., et. al 2009, A&A, 494, 127
Schmidt, W., Federrath, C., & Klessen, R. 2008, Phys. Rev. Lett., 101, 194505
Ustyugov, S. D., Popov, M. V., Kritsuk, A. G., & Norman, M. L. 2009, JCP, submitted
von Kármán, T. & Howarth, L. 1938, Proc. Roy. Soc. London, Ser. A, 164, 192
Yousef, T. A., Rincon, F., & Schekochihin, A. A. 2007, J. Fluid Mech., 575, 111